

Assessment of the Effect of Dimethyl Disulfide Concentration Dosing on Coke Formation and Furnace Run Length Predictions: Experimental and Modeling Study

Ali Darvishi* and Razieh Davand

Research and Development Center, Jam Petrochemical Company, Asaluyeh, Bushehr, Iran
Department of Chemical Engineering, School of Chemical and Petroleum Engineering, Shiraz University, Shiraz, Iran

Somayah Mohebi, Akbar Bolhasani, Soroush Karamian, Shahin Hosseini, Reza Rashedi, Ourmazd Dehghani and Aghil Parvin

Research and Development Center, Jam Petrochemical Company, Asaluyeh, Bushehr, Iran

* Corresponding author. E-mail: Ali.darvishi@jpcomplex.com DOI: 10.14416/j.asep.2022.09.001

Received: 28 March 2022; Revised: 28 May 2022; Accepted: 19 July 2022; Published online: 2 September 2022

© 2022 King Mongkut's University of Technology North Bangkok. All Rights Reserved.

Abstract

The olefins are produced by steam cracking furnaces in the petrochemical industry. The olefins production is strongly affected by the furnace run length. The coke deposition inside the cracking coil determines the furnace run length. Dimethyl disulfide (DMDS) is mainly utilized in steam crackers as coke and CO inhibitors. A cracking setup is utilized for studying the influence of various concentrations of DMDS on cracking performance. The simulation model utilized to evaluate furnace run length showed excellent performance in the prediction of the furnace run length (average absolute error = 0.83%). The ethane conversion, ethylene selectivity, carbon monoxide (CO) formation, coking rate, coke morphology, and metal migration to coke are vital parameters in olefin performance and furnace run length. Accordingly, different concentrations of DMDS including the industrial dosage are selected, evaluated, and optimized by the experimental method. The results show that the minimum coke formation is achieved when the DMDS concentration is 20 ppmw, in which the coking rate for steam cracking is 52% less than that of industrial dosage (111 ppmw). Moreover, a 50% decrease in CO formation is observed when DMDS concentration changed from 111 to 20 ppmw. Based on the simulation model, the optimum DMDS dosage results in an increase in the run length from 60.21 to 95.12 days.

Keywords: Coke layer, Steam cracking, Coke rate, DMDS dosage, CO

1 Introduction

Nowadays, 70% of olefin production comes from steam cracking of various hydrocarbons in olefin plants, where propylene and ethylene are the main products of the process [1]. The ethylene and propylene production is strongly affected by the coke deposition inside the cracking coil, which determines the furnace run length. The coke and carbon monoxide (CO) formation are inevitable in a steam cracking process [2], [3]. The formation of the coke layer results in increased heat transfer resistance and detrimental effects

on the coil material due to hot spots and corrosion, respectively. Consequently, it reduces olefin yield and furnace run length [4], [5]. On the other hand, CO formation acts as a poison for the selective hydrogenation catalyst utilized in the downstream units. It reduces the efficiency of the pressure swing adsorption unit in an olefin plant [4], [6], [7].

Coke is generated through different mechanisms, which catalytic and pyrolytic mechanisms are the most important ones for light feed thermal cracking [8]. The catalytic mechanism takes place in the presence of hydrocarbon and active sites on the coil

surface (Fe and Ni). The radicals are formed in the reaction media of producing coke, which deposits on the coil surface (a pyrolytic mechanism). At the start of a run of steam cracking in the furnace, the metallic surface of cracking coils containing Fe-Ni works as an active site and enhances coke deposition. Thus, the predominant mechanism is catalytic. However, after coke deposition, the catalytic activity of the coil alloy is minimized, and the pyrolytic mechanism becomes the prevailing one. Pyrolytic coke formation involves reactions between coke precursors in the gas phase (unsaturated hydrocarbons, aromatics, free radicals) and the coke surface. Most of the coke formed in the radiant section is pyrolytic, leading to more growth of the catalytic coke layer [8], [9].

Furthermore, CO formation is tied to the thermal oxidation of coke by steam. However, contradicting theories suggest that the quantity of CO is not always a measure of the amount of coke formed in the cracking process [4], [6], [10].

The coke and CO formation inhibition depend on various factors, including feed quality, operating conditions, coil material, and coke inhibitor type [4], [9]. Therefore, due to each olefin plant's unique coil material, feed impurities, and operating conditions, the coke inhibitor type and dosage are the primary methods to avoid coke and CO formation. To do so, dimethyl disulfide (DMDS), with its heteroatom elements that block the catalytic active sites on the surface of the coil alloy, is mainly utilized in steam crackers to reduce coke formation [11]–[15]. Under cracking temperature, DMDS decomposes into H_2S , which plays the major coke inhibiting function [9], [14], [16]. It inhibits the catalytic effects of iron, nickel, and other metal elements and reduces catalytic coke formation. Additionally, it terminates free radicals and inhibits pyrolytic mechanisms [17]–[19].

In most industrial plants, the protocol for DMDS injection includes initial sulfidation followed by continuous addition of the inhibitor. For the continuous injection of DMDS, two contradictory roles are reported that affect the rate of coke formation: A promoting effect of hydrogen sulfide via facilitating the adsorption of hydrocarbon radicals on the metal surface and a reduced catalytic effect of the metal surface via sulfidation. This implies that the concentration of the DMDS in the feed stream has to be carefully determined. An optimized inhibitor injection dosage

should be employed to manage a profitable strategy and reduce inhibitor consumption in large-scale plants. For achieving this goal, there have been hitherto significant efforts toward the process simulation and experimental studies in both academic and industrial [20]–[24]. However, the previous studies shows that the influence of DMDS continuous injection on the performance of a cracking furnace is inconsistent, and the scattered data reported in the literature do not precisely support one another (Table 1). Additionally, the sources of the observed effects are not fundamentally clear [25], [26]. In other words, although DMDS acts positively as a coke inhibitor with heavy feeds, such as naphtha, it may show an unexpected behavior with light feeds, such as ethane [25]–[27]. This unexpected behavior necessitates the investigation of the impact of DMDS in further studies. It is thus evident that the observations made for coking during gas feed cracking cannot be simply translated to liquid cracking. Hence, there is a clear need for a detailed study of continuous DMDS introduction to ethane furnace crackers, including an investigation of the coking rate, CO formation, coke morphology, metal migration, ethane conversion, ethylene selectivity, and furnace run length in ethane steam cracking, simultaneously. Additionally, the mass, energy, momentum balance, cracking reaction, and coke formation kinetic should be needed to predict the furnace run length.

Table 1: The influence of DMDS continuous injection enhancement on coking rate

Feed	Coking Rate	References
n-nonane	Increase	[28]
n-hexane	Increase	[27]
Naphtha	Reduction	[29]
Naphtha	Reduction	[28]
Propane	Reduction	[30]

The present study is devoted to optimizing the DMDS continuous injection dosage. To find an optimized DMDS injection dosage, decision variables including coke deposition, CO formation, ethane conversion, and ethylene selectivity are examined under several DMDS concentrations (0–150 ppmw). These experimental tests allowed us to find the best DMDS dosage to reduce the quantities of coke and CO formation in an existing large-scale production plant. It also provides an insight into the effect of DMDS on the furnace run length.

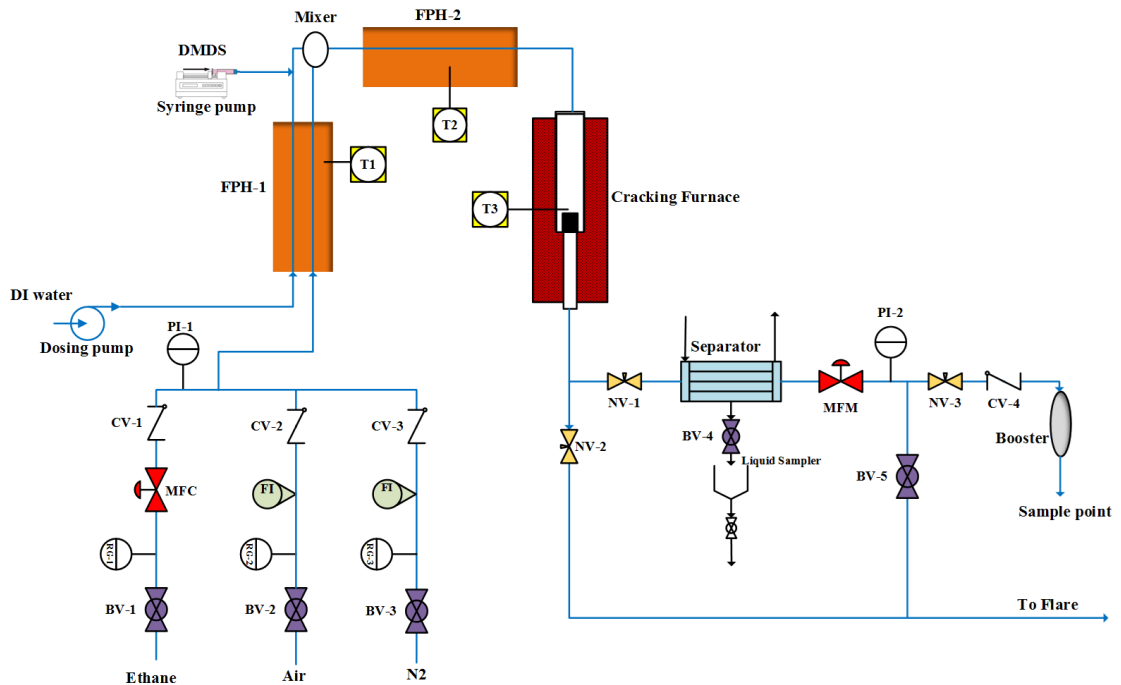


Figure 1: Schematic representation of steam cracking experimental apparatus.

2 Materials and Methods

2.1 Chemical materials

Ethane and DMDS are supplied from the JAM petrochemical plant in Iran. Coupons were fabricated from an HP40 with $2 \times 11 \times 14.8$ mm, which were cut out of the inner side of the industrial steam cracking coil. According to EDAX analysis, the fresh HP40 alloy is mainly composed of 23–25 %wt. Chromium, 33–38%wt. Nickel, 1–1.5 %wt. Manganese and 1–2%wt. Silicon, respectively. In order to analyze the coke formed over cracking runs, the coupons were placed in the tubular reactor which was constructed from SS309.

2.2 Characterization of samples

The coke layer formed on the coupon surface was characterized by a scanning electron microscope (SEM) to investigate the surface morphology and metal compositions within the coke layer. A Tescan MIRA3 device was used to collect the SEM data of the coupons, which was equipped with an energy-dispersive X-ray analyzer (EDAX).

2.3 Apparatus

To investigate and optimize the DMDS dosage, a set of ethylene cracking experimental equipment is designed and established in the JAM petrochemical laboratory, including the feed section, hot section, and coil section (Figure 1).

Feed section: Ethane flowrate is regulated by a Brooks mass flow controller. Steam is generated by injecting deionized water with a syringe pump into an FPH-1 which is set at 130 °C. The syringe pump, ISCO 500D, has already been calibrated with a volumetric flask (+0.1 mL) and a stopwatch for DMDS injection. Nitrogen and air flow rates are adjusted by two bubble flow meters. Check valve and pressure indicators control the pressure throughout the gas lines.

Hot section (cracking section): Deionized water and ethane are first fed to the feed preheater (FPH-1). DMDS is added to steam before getting into the mixer. The ethane and steam blend is then passed to a spiral mixer located upstream (FPH-2) to ensure proper mixing. The second preheater increases the temperature to 650 °C before the feed enters the cracking reactor. The FPH-1, FPH-2, and cracking furnaces are made up of copper

coils heated electrically, and electronic controllers adjust their temperatures. The reactor temperature is sensed with a K-type thermocouple placed on the coupon. The reactor, FPH-1, and FPH-2 are preoxidized with air at 650–700 °C to completely remove previously deposited coke. Once the peroxidation period is finished, nitrogen purges the setup while the temperature rises to 845 °C. This temperature is the preferred cracking temperature.

Cold section: The reactor effluent passes through a separator located immediately after the reactor to cool down the effluent and condense the remaining steam. Then, the cracked gas is sent for analysis in a gas chromatographer (SPSIC GC112A) equipped with a thermal conductivity detector (TCD) for detection of permanent gases and a flame ionization detector (FID) for detection of C1 to C10 hydrocarbons, and sulfur conductivity detector (SCD) for detection H₂S was utilized (4 mm ϕ stainless steel packed column: Propak Q, with 2 m length).

2.4 Scale down method

Scale downing is performed by utilizing two-dimensional equations governing the ethane steam cracking obtained from mass, energy, and momentum balances and then converting them to dimensionless form by unifying the expression related to convection in the direction axis. A complete list of similarity criteria can be obtained. The Euler number (Eu) is a critical similarity criterion in the steam cracking process [31]. The rationale behind this choice is further presented in the literature [31]. Finally, the scale-down relationships for the steam cracking process are Equations (1) and (2):

$$\frac{F_E}{F_I} = \left(\frac{d_E}{d_I} \right)^{\frac{29}{12}} \quad (1)$$

$$\frac{L_E}{L_I} = \left(\frac{d_E}{d_I} \right)^{\frac{5}{12}} \quad (2)$$

where F is the ethane mass flow rate, d is the coil diameter, L is the coil length, and the indices E and I represent the experimental and industrial scales, respectively.

Table 2 summarizes the scale-down result and

the complete operating conditions are summarized in Table 3. The reason for choosing a time of 60 min is that the highest coking rate and CO formation are at the beginning of cracking, and then they decrease [25]. Moreover, the ethane cracking process is at its worst case in terms of CO formation and coking rate at the beginning of steam cracking. It should be mentioned that the catalytic mechanism is also predominant in this period.

Table 2: Scale-down result

Parameter	Unit	Industrial scale	Experimental scale
Flow	[ml/h]	381292	3500
Inlet diameter	[cm]	9.5–11.5	0.08–0.12
Length	[m]	72	0.58

Table 3: Operating condition of cracking reaction

Parameters	Unit	value
Ethane flow rate [□]	ml/h	3500
Steam to ethane ratio*	wt./wt.	0.3
Cracking time ⁺	min	60
Preheater temperature (FPH-1)*	°C	130
Preheater temperature (FPH-2)*	°C	650
Cracking temperature*	°C	845
DMDS dosage range*	ppmw	0–150

[□] Scale down, * Industrial condition, ⁺ Literature [25]

3 Results and Discussion

The cracking system containing DMDS, steam, and ethane was studied over the range of 0 (blank) to 150 ppmw DMDS in ethane and steam streams. To ensure repeatability, the tests were carried out three times. Then, the rate of coke formation, morphology, metal migration from coupon surface, ethane conversion, and ethylene selectivity were examined.

3.1 Conversion and selectivity

Ethane conversion and ethylene selectivity are two essential parameters analyzed under different DMDS concentrations. It is preferable that the addition of coke inhibitor decreases the coke formation without significantly affecting the ethane conversion and ethylene selectivity. In this regard, gas product samples were analyzed by GC to find the amount of ethane residual and ethylene in the effluent gas stream. Ethane conversion and selectivity are calculated by

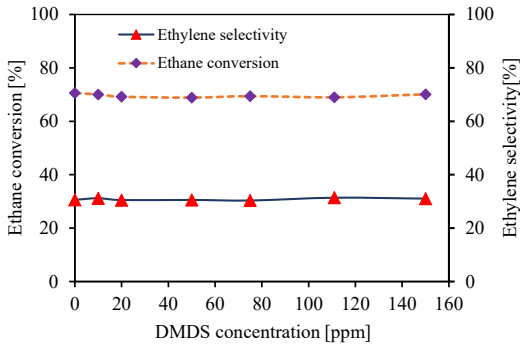


Figure 2: The effect of DMDS concentration on ethane conversion and ethylene selectivity.

Equations (3) and (4), and the results are plotted in Figure 2.

As it can be seen, the DMDS dosage does not affect ethane conversion and ethylene selectivity. The results obtained are also in good agreement with the literature [32].

$$\text{Ethane conversion (\%)} = \frac{F_{\text{Ethane}}^{\text{In}} - F_{\text{Ethane}}^{\text{Out}}}{F_{\text{Ethane}}^{\text{In}}} \times 100 \quad (3)$$

$$\text{Ethylene selectivity (\%)} = \frac{F_{\text{Ethylene}}^{\text{Out}}}{F_{\text{Ethane}}^{\text{In}}} \times 100 \quad (4)$$

Thus, it is feasible to optimize the DMDS dosage based on the coking rate and CO formation without worrying about the adverse effects of the optimum DMDS dosage on the total conversion and yield of the steam cracking.

3.2 Coke formation

In each test, the rate of coke deposition over the metal surface of coupons is calculated by Equation (5) [18].

$$\text{Coking rate} \left(\frac{\text{mg}}{\text{m}^2 \cdot \text{s}} \right) = \frac{m_{\text{final}} - m_{\text{initial}}}{\text{cracking time} \times A_{\text{coupon}}} \quad (5)$$

where m_{initial} and m_{final} denote the mass of the coupon before and after each cracking test, respectively. A_{coupon} is the coupon area (m^2), and t_c is the cracking time (s).

The averaged results of the tests are shown in Figure 3. As shown in Figure 3, the coking rate on coupons is strongly affected by DMDS dosage and the rates of coke deposition are 82.88 and 18.13 $\text{mg}/\text{m}^2\text{s}$

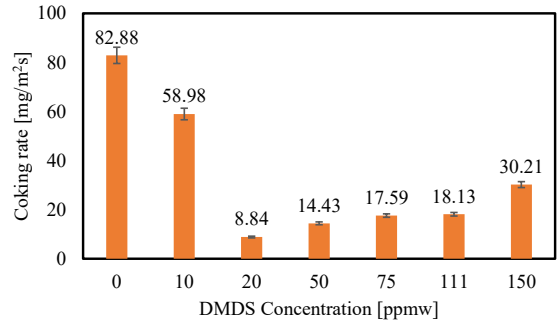


Figure 3: Coking rate as a function of DMDS concentration.

for the blank feed (0 ppmw) and 111 ppmw (industrial dosage) of DMDS, respectively. Moreover, it is obvious that increasing DMDS dosage up to 20 ppmw leads to a significant decrease in the coking rate (8.84 $\text{mg}/\text{m}^2\text{s}$). In contrast, injection of more concentrations of DMDS leads to a gradual increase in the coking rate. In fact, at 20 ppmw DMDS concentration, the coke deposition rate is at the lowest value. While, at two extremes, the blank and industrial dosage of DMDS, the coking rate is considerably high. In fact, the coking rate in the optimal dosage (20 ppmw) is reduced by 52% compared to the industrial dosage (111 ppmw).

The continuous injection of 20 ppmw DMDS creates a sufficient layer of sulfide on the coil surface to control the catalytic mechanism. The amount of H_2S formation under different DMDS dosages is depicted in Figure 4, which justifies the importance of the optimum dosage of the coke inhibitors. In other words, the DMDS dosage that is higher than the optimal value (greater than 20 ppmw) leads to further production of excess H_2S compounds. The excess H_2S causes the formation of HS^\cdot radicals that interfere with heterogeneous non-catalytic radical reactions and contribute to increasing asymptotic coke formation and growth of the coke layer [4], [8], [33].

The adverse effects of the DMDS inhibitor, when added in excess, can be observed in the results shown in Figure 3. This trend agrees well with the previous studies' observations, which show that injection of DMDS more than 20 ppmw results in an increase in coke formation [33]. It could be concluded that the low amount of DMDS (H_2S) decreases the catalytic coking mechanism, while the excess DMDS (H_2S) increases the pyrolytic coking mechanism [34].

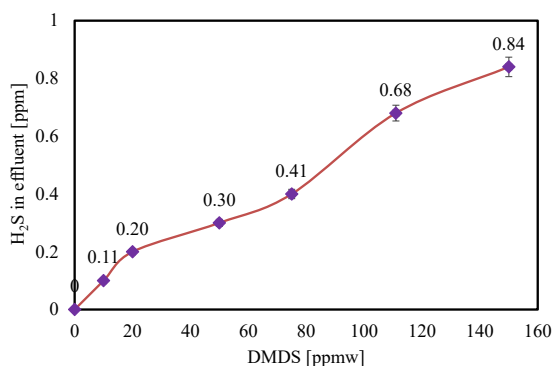


Figure 4: H₂S in effluent as a function of DMDS concentration.

3.3 CO formation

The amount of CO formation under different DMDS dosages is evaluated and the results are depicted in Figure 5. It can be seen that the concentration of CO in the effluent at the blank (0 ppmw) and industrial (111 ppmw) injection dosages are 11366 and 4019 ppmw, respectively. Additionally, based on the experimental observations, 10 ppmw of DMDS is accompanied by the lowest amount of CO formation. Additionally, the CO concentration rises slowly with increasing DMDS dosage from 20 to 150 ppmw. In steam cracking, two processes contribute in the production of CO. The metal-catalyzed removal of coke by steam reforming and gasification of coke by steam. As the active sites play the catalytic role for the water gas shift reaction, they are covered and deactivated by the small amounts of DMDS and therefore, the low amount of DMDS results in a reduction of CO production. However, it was shown that a higher amount of continuously added DMDS is associated with higher coke formation. As a result, the metal surface becomes covered by coke and its catalytic activity diminishes. Therefore, CO production is only related to the rate of coke formation in higher DMDS concentrations and it increases with increasing the amount of DMDS. At the same time, the excess dosage of steam contributes to the coke formation in the pyrolytic mechanism. Consequently, coke can be converted to CO by gasification reaction ($C + H_2O \rightarrow CO + H_2$) [35], [36]. The results show good agreement with the previous study [33]. Considering the simultaneous impacts of DMDS concentration on CO formation and coke deposition, it is essential to

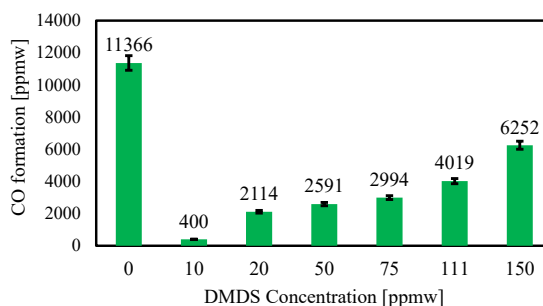


Figure 5: Carbon monoxide formation versus DMDS concentration.

make a balance to find the optimum value of DMDS dosage. In this regard, the coke deposition rates are 58.98 and 8.84 mg/m²s, while the CO concentrations are 400 and 2114 ppmw at DMDS values of 10 and 20 ppmw, respectively. Although 10 ppmw DMDS leads to the lowest CO formation, the coking rate is considerably high. On the other hand, adjusting DMDS concentration to 20 ppmw results in the lowest coking rate while it is accompanied by a minor increase in CO concentration. It is worth mentioning that the CO formation and coking rate under the current industrial dosage are 4019 ppmw and 18.13 mg/m².s, respectively. Due to the fact that coke formation has more negative effects on the run length of the current cracking furnace than CO formation, 20 ppmw would be the optimum for DMDS injection.

3.4 SEM and EDAX analysis

The morphologies of the coke layers of the samples for the industrial and optimum DMDS dosage were evaluated using SEM technique [37], [38]. The corresponding results are demonstrated in Figure 6. It is obvious that the dimension and population of the coke filaments of the current industrial case (111 ppmw) do not show significant change compared to those of the optimum point (20 ppmw) and it can be said that the morphology of the coke layer is almost independent of DMDS dosage.

Furthermore, EDAX analysis has been carried out on the coke layer to evaluate the effectiveness of DMDS concentration in preventing metal migration [5], [39]. Figure 7 illustrates the metal content of the coke layer formed over ethane cracking with new (20 ppmw) and industrial (111 ppmw) dosages of

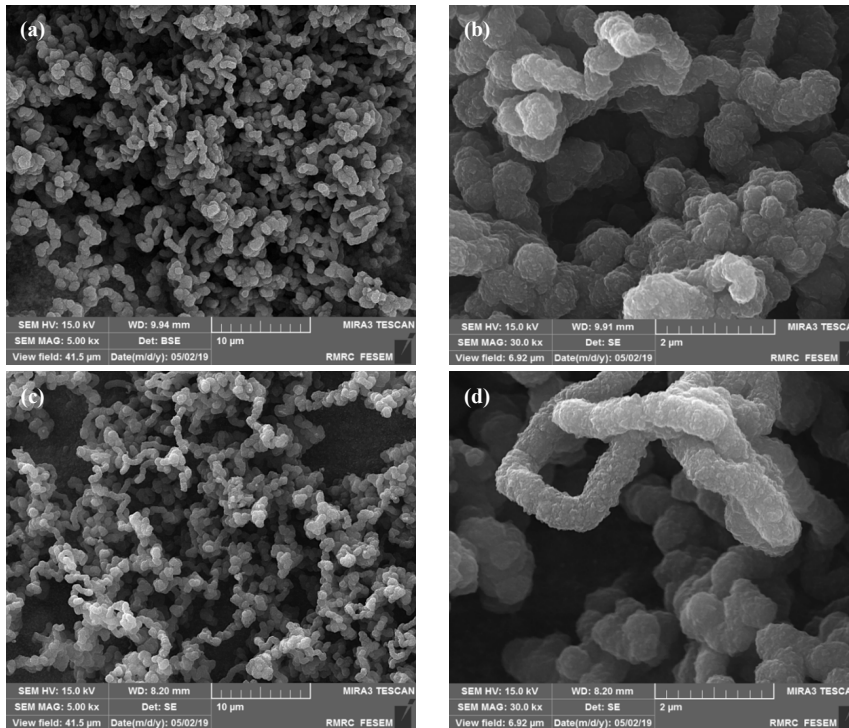


Figure 6: SEM images of the surface of (a) and (b) a coupon of industrial protocol and (c) and (d) a coupon of new protocol; Magnification: 10 µm (a), (c); 2 µm (b), (d).

DMDS. The results presented in Figure 7 show a depletion of chromium and iron in the coke formation of the new dosage compared to the industrial dosage, accompanied by an increase in manganese, niobium, and nickel. In general, performing a new DMDS injection dosage decreases the metal migration from the coupon surface. It can be seen that the amount of metal in the coke layer at the optimum dosage (20 ppmw) and industrial (111 ppmw) injection dosages are 24.5 and 26.7%, respectively. Therefore, according to minimum coking rate and CO formation, ethane conversion, and ethylene selectivity, 20 ppmw of DMDS is the most appropriate concentration for the injection in the olefin plant. In the following step, the effect of injection of the optimal amount of DMDS (20 ppmw) on the run length of the cracking furnace is investigated.

3.5 Simulation of the run length with the new DMDS dosage injection

In the previous work [2], a simulation model for

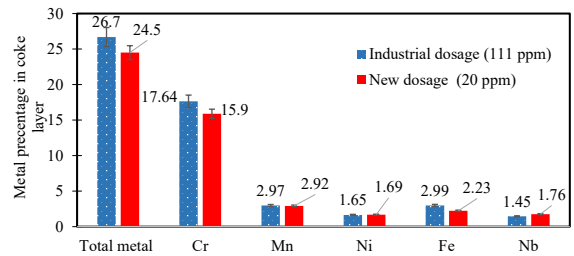


Figure 7: The metal composition of the coke layers formed in the industrial (111 ppmw) and the new (20 ppmw) DMDS injection dosage.

steam cracking of ethane was developed in MATLAB programming medium and the semiempirical Hernandez (model 1) [40] and Van Geem (model 2) [41] models were used to simulate the coking rate. In order to verify the accuracy of the simulation model, the results are compared with the plant data. In this regard, five cycles of steam cracking in the industrial furnace (from start up to end of run) were used for model validation. Five different feed compositions at

various operating conditions are injected into the cracking furnace (Table 4). The details of the simulation and real run length of five cases are well provided in Table 5. Additionally, in order to compare the model result with the real olefin plant data, absolute error is calculated by Equation (6) and the results are summarized in Table 5. In order to compare the model result with the real olefin plant data, absolute error is calculated by Equation (6) and the results are summarized in Table 5.

$$\text{Absolute error (\%)} = \frac{\text{Exp.} - \text{Calc.}}{\text{Exp.}} \times 100 \quad (6)$$

It can be seen that both simulation models exhibit a promising performance in predicting industrial condition in all cases and they could evaluate furnace run length with acceptable accuracy and the average absolute error for these five cases is calculated to be 1.36 and 0.83 for model 1 and model 2, respectively. However, as model 2 considered the combined effect of catalytic and pyrolytic coke formation in its coke rate simulation, it accompanied by less average absolute error and therefore a better performance in simulating coking rates.

The calculated furnace run lengths versus DMDS concentration are shown in Figure 8. It is known that the more coke formation, the less run length of the furnace. The coke deposition along the length of coils increases the thermal resistance and therefore it is accompanied by a decrease in the rate of heat transfer. As a result, the formation of coke leads to an increase

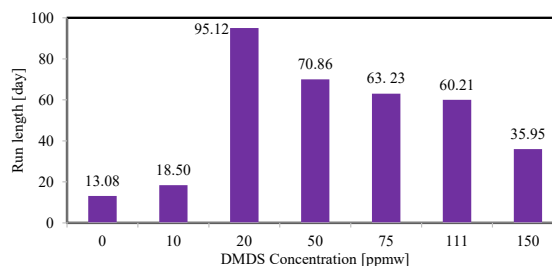


Figure 8: The influence of DMDS concentration on the furnace run length formation.

in skin temperature and pushes the furnace conditions towards shutting down criteria, which are adjusted to be 1110 K and 0.94 for the coil skin temperature and coil outlet pressure to coil inlet pressure ratio in the venturi nozzle, respectively [42]. As shown in Figure 8, the simulation model can effectively simulate the influence of DMDS dosage on the amount of coke deposited and therefore furnace run length and applying 20 ppmw of DMDS increases the cracking furnace run length from 60.21 in the industrial case to 95.12 days, which confirms the results demonstrated in Figure 4. It should be mentioned that according to the results shown in Figure 4, performing the new DMDS dosage (20 ppmw) decreases the coke formation by approximately 52% which reflects 58% increment in the cracking furnace run length in comparison with industrial DMDS dosage (111 ppmw). Moreover, one can be concluded from Figure 8 that increasing the DMDS concentration is not suggestive of an increase

Table 4: Feed compositions and operating conditions of five industrial cracking furnaces

Property	Unit	Case 1	Case 2	Case 3	Case 4	Case 5
Feed composition (ethane/propane)	wt. %	100/0	95/5	90/10	80/20	100/0
Feed flow rate	ton/h	40	40	40	40	28
Furnace temperature	K	1514.15	1510.15	1505.25	1495.45	1459.05
Feed temperature	K	947.25	941.34	933.75	919.14	857.42
Feed pressure	bar	2.98	2.97	2.96	2.94	2.81
Steam ratio	kg steam/kg feed	0.300	0.300	0.300	0.300	0.625

Table 5: Comparison between model result and real olefin plant data in five industrial cases

		Case 1	Case 2	Case 3	Case 4	Case 5
Industrial data		64.75	75.04	90.33	132.71	174.25
Model 1	run length (day)	64.10	74.21	88.88	134.04	170.59
	Absolute error	1	1.1	1.6	1	2.1
Model 2	Run length (day)	64.3	74.81	89.05	131.65	175.85
	Absolute error	0.69	0.3	1.42	0.8	0.92

in run length and as the DMDS concentration is increased, the furnace run length first increased up to 20 ppmw DMDS and then it is decreased by increasing DMDS dosage from 20 to 111 ppmw.

It is well-known that DMDS plays two roles in coke formation [41]. Firstly, it covers the metal surface of the coils and prevents the reaction between hydrocarbons and the metal particles of the surface, which act as active sites to catalyze the filamentous coke formation. The more DMDS concentration reduced coke formation through a heterogeneous catalytic mechanism [43]. Secondly, DMDS is effective in the formation of HS[·] radicals through a pyrolytic mechanism. These radicals represent the contradictory effect on heterogeneous non-catalytic coke formation mechanism. The formed HS[·] radicals react with a surface layer of coke and reduce coke deposition. However, if more radicals are present than the active surface of coke, they may participate in the reaction with hydrocarbons and causing the hydrocarbons to grow and turning them into heavier hydrocarbons, which deposit on the coil surface and results in an increase in coke layer thickness. As a result, it would be concluded that 20 ppmw is well-selected as the optimum DMDS dosage.

4 Conclusions

The role of DMDS concentration on coke formation in ethane steam cracking at industrially representative conditions was assessed by experimental and simulation methods. In this regard, the DMDS injecting dosages were adjusted over the range of DMDS 0 to 150 ppmw and a cracking setup was used for studying the influence of various concentrations of DMDS on ethane conversion, ethylene selectivity, CO formation, coking rate, coke morphology, and metal content in the coke layer. The experimental results revealed that coke deposition and CO formation are strongly affected by the DMDS concentration. Due to these results, the 20 ppmw is optimum concentration for DMDS injection. Addition of 20 ppmw DMDS significantly prevents coke and CO formations. In this optimum DMDS dosage, coking rate, CO production, and metal migration were decreased 52%, 50%, and 2.2%, respectively. The reduction in the coking rate is 52% by optimum DMDS dosage. Accordingly, simulation of ethane steam cracking by MATLAB R2019a revealed that applying the optimum

DMDS dosage increases the run length of the reactor from 60.21 to 95.12 days. This means that the increase in run length would be up to 58%.

Author Contributions

A.D.: conceptualization, experimental design, writing original draft, reviewing and editing; S.M.: experimental design; A.B.: conceptualization, supervision; S.K.: experimental design; S.H.: investigation, reviewing and editing, supervision; R.D.: conceptualization, writing original draft, reviewing and editing; R.R.: conceptualization; O.D.: industrial advisor; A.P.: industrial advisor. All authors have read and agreed to the published this version of the manuscript.

Conflicts of Interest

The authors declare no conflict of interest.

References

- [1] H. Mizuma, M. Nakatsu, and Y. Iwama, "A study on remote fracturing system using the steam pressure cracking agent," in *the Proceedings of Mechanical Engineering Congress Japan*, 2019, doi: 10.1299/jsmemecj.2019.S08112.
- [2] Z. Feli, A. Darvishi, A. Bakhtyari, M. R. Rahimpour, and S. Raeissi, "Investigation of propane addition to the feed stream of a commercial ethane thermal cracker as supplementary feedstock," *Journal of the Taiwan Institute of Chemical Engineers*, vol. 81, pp. 1–13, 2017.
- [3] L. Ortiz, K. Yang, and B. Church, "Performance of alumina-forming alloys under coking–decoking cycles," *Industrial & Engineering Chemistry Research*, vol. 59, no. 25, pp. 11485–11493, 2020.
- [4] I. Kucora, P. Paunjoric, J. Tolmac, M. Vulovic, J. G. Speight, and L. Radovanovic, "Coke formation in pyrolysis furnaces in the petrochemical industry," *Petroleum Science and Technology*, vol. 35, no. 3, pp. 213–221, 2017.
- [5] M. Patil, S. A. Sarris, K. Verbeke, M.-F. Reyniers, and K. M. V. Geem, "Catalytic effect of dimethyl disulfide on coke formation on high-temperature alloys: Myth or reality?," *Industrial & Engineering Chemistry Research*, vol. 59, no. 34, pp. 15165–15178, 2020.

- [6] A. E. M. Gandarillas, K. M. V. Geem, M.-F. Reyniers, and G. B. Marin, "Influence of the reactor material composition on coke formation during ethane steam cracking," *Industrial & Engineering Chemistry Research*, vol. 53, no. 15, pp. 6358–6371, 2014.
- [7] A. Hafizi, M. Rahimpour, P. Pakdaman, A. Darvishi, and A. Bolhassani, "Experimental investigation of coke deposition in the structure of Pd-Ag/ α -Al₂O₃ industrial catalyst," *Nashrieh Shimi va Mohandesi Shimi Iran*, to be published, 2020.
- [8] M. P. Bukhovko, L. Yang, I. Nezam, L. Li, A. Malek, R. J. Davis, P. K. Agrawal, and C. W. Jones, "Enhanced coke gasification activity of the Mn_{1.5}Cr_{1.5}O₄ spinel catalyst during coking in ethylene–steam mixtures," *Energy & Fuels*, vol. 35, no. 6, pp. 5271–5280, 2021.
- [9] G. F. Glasier and P. D. Pacey, "Formation of pyrolytic carbon during the pyrolysis of ethane at high conversions," *Carbon*, vol. 39, no. 1, pp. 15–23, 2001.
- [10] D. Salari, A. Niaei, M. R. Shoja, and R. Nabavi, "Coke formation reduction in the steam cracking of naphtha on industrial alloy steels using sulfur-based inhibitors," *International Journal of Chemical Reactor Engineering*, vol. 8, no. 1, 2010, doi: 10.2202/1542-6580.2304.
- [11] S. Sadrameli, "Thermal/catalytic cracking of hydrocarbons for the production of olefins: A state-of-the-art review I: Thermal cracking review," *Fuel*, vol. 140, pp. 102–115, 2015.
- [12] M. Geerts, S. H. Symoens, P. A. Reyniers, G. B. Marin, M.-F. Reyniers, and K. M. V. Geem, "Steam cracking coke properties and their influence on furnace run length predictions: experimental and modeling study," *Industrial & Engineering Chemistry Research*, vol. 59, no. 52, pp. 22460–22472, 2020.
- [13] M. Mobaraki, B. Afshang, M. Rahimpour, M. Bahrololoom, A. Bolhasani, and R. Davand, "Effect of cracking feedstock on carburization mechanism of cracking furnace tubes," *Engineering Failure Analysis*, vol. 107, 2020, Art. no. 104216.
- [14] A. Goswami and S. Kumar, "Failure of pyrolysis coils coated with anti-coking film in an ethylene cracking plant," *Engineering Failure Analysis*, vol. 39, pp. 181–187, 2014.
- [15] S. A. Sarris, S. H. Symoens, N. Olahova, K. Verbeken, M.-F. Reyniers, G. B. Marin, and K. M. V. Geem, "Impact of initial surface roughness and aging on coke formation during ethane steam cracking," *Industrial & Engineering Chemistry Research*, vol. 56, no. 44, pp. 12495–12507, 2017.
- [16] S. H. Symoens, N. Olahova, A. E. M. Gandarillas, H. Karimi, M. R. Djokic, M.-F. Reyniers, G. B. Marin, and K. M. V. Geem, "State-of-the-art of coke formation during steam cracking: Anti-coking surface technologies," *Industrial & Engineering Chemistry Research*, vol. 57, no. 48, pp. 16117–16136, 2018.
- [17] D. Brown, J. Clark, A. Foster, J. McCarroll, and M. Sims, "Inhibition of coke formation in ethylene steam cracking," *ACS Publications*, vol. 2, pp. 23–43, 1983.
- [18] X. Ding, Z. Wang, B. Wang, and Z. Xing, "The effects of sulfides and sulfur/phosphorus-containing compounds on coke formation during thermal cracking of light naphtha," *Asia-Pacific Journal of Chemical Engineering*, vol. 16, no. 1, 2021, Art. no. e2573.
- [19] N. I. Olahová, S. H. Symoens, M. R. Djokic, N. D. Ristic, S. A. Sarris, M. Couvrat, F. Riallant, H. Chasselin, M.-F. Reyniers, and K. M. V. Geem, "CoatAlloy barrier coating for reduced coke formation in steam cracking reactors: Experimental validation and simulations," *Industrial & Engineering Chemistry Research*, vol. 57, no. 3, pp. 897–907, 2018.
- [20] K. Bi, B. Beykal, S. Avraamidou, I. Pappas, E. N. Pistikopoulos, and T. Qiu, "Integrated modeling of transfer learning and intelligent heuristic optimization for a steam cracking process," *Industrial & Engineering Chemistry Research*, vol. 59, no. 37, pp. 16357–16367, 2020.
- [21] A. Darvishi, M. R. Rahimpour, and S. Raeissi, "A theoretical and experimental study for screening inhibitors for styrene polymerization," *Processes*, vol. 7, no. 10, 2019, Art. no. 677.
- [22] R. Davand, M. R. Rahimpour, S. Hassanajili, and R. Rashedi, "Theoretical and experimental assessment of UV resistance of high-density polyethylene: Screening and optimization of

- hindered amine light stabilizers,” *Journal of Applied Polymer Science*, vol. 138, no. 43, 2021, Art. no. 51262.
- [23] H. Aammer, Z. M. Shakor, F. Al-Sheikh, S. A. Al-Naimi, and W. A. Anderson, “Simulation and optimization of the ethane cracking furnace using ASPEN PLUS and MATLAB: A case study from petrochemical complexes,” *Combustion Science and Technology*, 2022, doi: 10.1080/00102202.2022.2029854.
- [24] K. K. Parmar, G. Padmavathi, S. K. Sharma, and R. Jasra, “Effect of sulfur additives on coke formation during steam cracking of naphtha,” *Journal of Chemical Sciences*, vol. 133, no. 4, 2021, Art. no. 121.
- [25] J. Wang, M.-F. Reyniers, K. M. V. Geem, and G. B. Marin, “Influence of silicon and silicon/sulfur-containing additives on coke formation during steam cracking of hydrocarbons,” *Industrial & Engineering Chemistry Research*, vol. 47, no. 5, pp. 1468–1482, 2008.
- [26] G. Hay, G. Rasouli, L. Carboognani-Arambarri, R. Suzuki, K. Urata, and M. Inoue, “Reduce coke formation and save operating costs with optimization of DMDS into ethane cracking furnaces,” *Hydrocarbon processing*, vol. 2, no. 1, pp. 49–52, 2017.
- [27] M.-F. Reyniers and G. F. Froment, “Influence of metal surface and sulfur addition on coke deposition in the thermal cracking of hydrocarbons,” *Industrial & Engineering Chemistry Research*, vol. 34, no. 3, pp. 773–785, 1995.
- [28] D. Depeyre, C. Flicoteaux, and J. G. Ossebi, “Pure n-nonane steam cracking and the influence of sulfur compounds,” *Industrial & Engineering Chemistry Process Design and Development*, vol. 24, no. 4, pp. 920–924, 1985.
- [29] I. Dhuyvetter, M.-F. Reyniers, G. F. Froment, G. B. Marin, and D. Viennet, “The influence of dimethyl disulfide on naphtha steam cracking,” *Industrial & Engineering Chemistry Research*, vol. 40, no. 20, pp. 4353–4362, 2001.
- [30] M. Patil, M. Djokic, K. Verbeken, M.-F. Reyniers, and K. M. V. Geem, “Effect of phosphine on coke formation during steam cracking of propane,” *Materials*, vol. 14, no. 17, 2021, Art. no. 5075.
- [31] R. Karimzadeh and M. Ghashghae, “Design of a flexible pilot plant reactor for the steam cracking process,” *Chemical Engineering & Technology: Industrial Chemistry-Plant Equipment-Process Engineering-Biotechnology*, vol. 31, no. 2, pp. 278–286, 2008.
- [32] D. L. Trimm and C. J. Turner, “The pyrolysis of propane. II. Effect of hydrogen sulphide,” *Journal of Chemical Technology and Biotechnology*, vol. 31, no. 1, pp. 285–289, 1981.
- [33] J. Wang, M.-F. Reyniers, and G. B. Marin, “Influence of dimethyl disulfide on coke formation during steam cracking of hydrocarbons,” *Industrial & Engineering Chemistry Research*, vol. 46, no. 12, pp. 4134–4148, 2007.
- [34] A. Singh, S. Paulson, H. Farag, V. Birss, and V. Thangadurai, “Role of presulfidation and H₂S cofeeding on carbon formation on SS304 alloy during the ethane–steam cracking process at 700 °C,” *Industrial & Engineering Chemistry Research*, vol. 57, no. 4, pp. 1146–1158, 2018.
- [35] I. Amghizar, J. N. Dedeyne, D. J. Brown, G. B. Marin, and K. M. Van Geem, “Sustainable innovations in steam cracking: CO₂ neutral olefin production,” *Reaction Chemistry & Engineering*, vol. 5, no. 2, pp. 239–257, 2020.
- [36] F. D. Kopinke, G. Zimmermann, G. C. Reyniers, and G. F. Froment, “Relative rates of coke formation from hydrocarbons in steam cracking of naphtha. 2. Paraffins, naphthenes, mono-, di-, and cycloolefins, and acetylenes,” *Industrial & Engineering Chemistry Research*, vol. 32, no. 1, pp. 56–61, 1993.
- [37] H. Cai, A. Krzywicki, and M. C. Oballa, “Coke formation in steam crackers for ethylene production,” *Chemical Engineering and Processing: Process Intensification*, vol. 41, no. 3, pp. 199–214, 2002.
- [38] D. Salari, A. Niaei, P. Panahi, R. Nabavi, and J. Toufighi, “Investigation of coke deposition & coke inhibition by organosulfur compounds in the pyrolysis of naphtha in the jet stirred reactor system,” *Iranian Journal of Chemical Engineering*, vol. 3, no. 1, pp. 40–51, 2006.
- [39] S. A. Sarris, M. Patil, K. Verbeken, M.-F. Reyniers, and K. M. V. Geem, “Effect of long-term high temperature oxidation on the coking behavior of Ni-Cr superalloys,” *Materials*, vol. 11, no. 10, 2018, Art. no. 1899.
- [40] A. Y. R. Hernandez, “A model for the prediction



- of olefin production and coke deposition during thermal cracking of light hydrocarbons,” Universidad Nacional de Colombia, Medellín, Colombia, 2012.
- [41] J. Zhang, R. Van de Vijver, I. Amghizar, M.-F. Reyniers, and K. M. V. Geem, “Combined catalytic and pyrolytic coking model for steam cracking of hydrocarbons,” *Industrial & Engineering Chemistry Research*, vol. 61, no. 11, pp. 3917–3927, 2022.
- [42] E. P. Schulz, J. A. Bandoni, and M. S. Diaz, “Optimal shutdown policy for maintenance of cracking furnaces in ethylene plants,” *Industrial & Engineering Chemistry Research*, vol. 45, no. 8, pp. 2748–2757, 2006.
- [43] D. Jakobi and P. Karduck, “Behavior of high-temperature tube materials in sulfur-containing steam-cracking conditions,” presented at the CORROSION 2018, Phoenix, Arizona, USA, Apr. 15, 2018.